Al-Nahrain Journal for Engineering Sciences **NJES** 28(1)52-60, 2025
http://doi.org/10.29194/NJES.28010052

A Review of Recent Studies in Microwave Photonics-based Filter Technologies: MRR-Assisted MZI Case Study

Esraa M. El-edresee[1], Alhuda A. Al-mfrji[2], Haider Al-Juboori[3]

Authors affiliations:
1) Department of Laser and Optoelectronics Engineering, College of Engineering, Al-Nahrain University, Baghdad, Iraq.
esraa.m.saeed@ced.nahrainuniv.edu.iq.

2*) Department of Laser and Optoelectronics Engineering, Al-Nahrain University, Baghdad, Iraq.
alhuda.a.oied@nahrainuniv.edu.iq.

3) South East Technological University, Faculty of Engineering, Department of Electronics Eng. & Com., Carlow, Ireland.
haider.aljuboori@setu.ie

Paper History:

Received: 12th May 2024

Revised: 28th June. 2024

Accepted: 4th Aug. 2024

Abstract

The recent progress in integrated photonics has promoted microwave photonic filter (MPF) technologies to a supreme level to develop wireless, radar, and internet communication systems. Thus, the tiny size, low power consumption, and low cost of the MPF chip are its unique features. By choosing the appropriate spectral content and rejecting sideband signals, the MPF made use of numerous technologies that proved the value of wide frequency tuning and reconfiguration in addition to its tolerance to electromagnetic interference. This paper reviews recent techniques involved in microwave filter design on multiple platforms, which involve cascaded micro-ring resonator (MRR), ring-assisted Mach-Zehender Interferometer (MZI) coupler, Brillion-active waveguide, reflector-type MRR, and Bragg grating with phase shifts. In particular, the output characteristics are demonstrated for the MRR integrated with a MZI coupler technique. The reviewed work will highlight the significant technological constraints and major technical limitations. Additionally, it suggests potential future directions for enhancing and optimizing microwave photonics-based filter technologies, which could pave the way for the next generation of communication systems.

Keywords: Microwave Photonic Bandpass Filter, Microring Resonator, Mach-Zehender Interferometer.

مراجعة للدراسات الحديثة في تقنيات الترشيح المعتمدة على الضوئيات بالموجات الدقيقة: دراسة حالة MZI بمساعدة MRR

اسراء محمد سعيد الادريسي، الهدى عبد الحسين المفرجي، حيدر الجبوري

الخلاصة:

أحدثت التطورات الأخيرة في مجال الضوئيات المتكاملة ثورة في تكنولوجيا المرشح الضوئي بالموجات الدقيقة (MPF) إلى حد غير مسبوق، مما أتاح بناء أنظمة الاتصالات اللاسلكية والرادار والإنترنت. وبالتالي، أصبح لشريحة MPF ميزات فريدة مثل الحجم الصغير والاستهلاك المنخفض للطاقة والتكلفة المنخفضة. ومن خلال اختيار المحتوى الطيفي المناسب ورفض إشارات النطاق الجانبي، استفادت MPF من العديد من التقنيات التي أثبتت قيمة ضبط الترددات الواسعة وإعادة تشكيلها بالإضافة إلى قدرتها على تحمل التداخل الكهرومغناطيسي. تستعرض هذه الورقة التقنيات الحديثة المستخدمة في تصميم مرشح الموجات الدقيقة على منصات متعددة، والتي تتضمن micro- (MRR) ring resonator،ring ، ومقرنة Mach-Zehender Interferometer (MZI) بمساعدة الحلقة، ودليل موجي نشط من نوع Brillion، وMRR من النوع العاكس، وتقنية Bragg grating. يتم توضيح خصائص الإخراج لـ MRR المتكامل مع تقنية مقرنة MZI. على وجه الخصوص. ستسلّط الدراسة الحالية الضوء على التحديات التكنولوجية المهمة والقيود التقنية الرئيسية. كما ستقترح الدراسة التوجهات المستقبلية المُحتملة لتحسين تقنيات المُرشّحات القائمة على فوتونيات الموجات الدقيقة، مما قد يُمهّد الطريق للجيل القادم من أنظمة الاتصالات.

1. Introduction

As the name signifies, the study of the interplay of microwave and optical signals for various purposes is known as microwave photonics, which is a multidisciplinary field], such as fiber-to-the-home, wireless communication, radar, sensors, broadband access networks, and filters [1-7]. The field of photonics emerged when scientists discovered that transmitting microwave signals in the electrical domain was challenging because of various factors, including bulkiness of the apparatus, heating effects, high losses at elevated frequencies, narrow bandwidth, and almost non-existent tunability of high-frequency filters [8]. Wilner and Van den

Heuvel's study was among the first to propose the use of optical fibers as delay lines to produce a photonic filter [9]. Microwave photonic filters became available in the development of this ground-breaking idea. Much work has been put into developing various microwave photonic filters in the last few years [10]. Significant benefits result from the employment of photonic components. For example, photonics-based microwave filters can be made tunable and programmable, which is a characteristic that is not feasible with conventional microwave technology [11]. Recent advancements in this field have shown that it is feasible to obtain filters with tuning ranges of 1 GHz to over 40 GHz, Q factors well above 10000 in the 2 and 10 GHz bands, and the capacity to reconfigure arbitrary transfer functions using electronic control signals in less time than 1 ms [12]. An abrupt slope in the transition band, excellent stop-band rejection, broad tunability [1,13], and a small flat-top bandpass [14,15], are among the most crucial and desired properties of microwave photonics (MWP) integrated optical filters [6]. Since this topic is gaining popularity, it is clear how challenging it is to simultaneously attain all these features given the narrow bandwidth of a filter operating at optical frequencies for the processing of microwave signals with sub-GHz resolution. Therefore, new technologies and networks for broadband wireless access—like 5G mobile wireless systems, local multipoint distribution services (LMDS), wireless local area networks (WLAN), and World Interoperability for Microwave Access (WIMAX)—require an increase in capacity by constricting the coverage area [10,6]. The literature has described a number of silicon photonics-based technology possibilities in depth, including: phase-shifted Bragg gratings, ring-loaded MZI topologies, and high-order micro-ring resonator MRR-based designs. Cascading different ring resonators together results in a higher insertion loss but sharper, narrower filtering in high-order MRRs [16]. An MZI configuration can be modified to create filters with varying shapes and perform the necessary signal shaping by incorporating MRRs [13]. Because of the nonlinear phase response of each arm of the MZI, small frequency bands across a large range can be eliminated [11]. Lately, several platforms have been used to design MPFs, including silicon on insulator (SOI) [17,18], silicon nitride [19,20], As2S3, indium phosphide [21], and lithium niobate. The most promising photonic integration platforms in recent times are those based on silicon photonics.

This paper focuses on the characteristics and features of different modern filter technologies that are used in the processing of microwave signals such as cascaded MRR, ring-assisted MZI coupler, reflector-type MRR, Brillion-active waveguide, and Bragg gratings. Many contemporary communications applications, including radar, optical networks, and satellites, take advantage of these features, which include vast tunability and reconfigurability as well as high rejection rates. Furthermore. the output property of the MZI coupler combined with the MRR design technology is thoroughly mathematically analyzed in this research paper. The concentrate on this technology was placed for several advantages, including power conservation, small size, and simple design that indicates a good option for designing MPF.

2. The general principle of MPF implementation

Photonic subsystems called microwave photonic filters are made to provide features that are either on par with traditional radio frequency (RF) systems or offer advantages unique to photonics, like low loss, immunity to electromagnetic interference (EMI), tunability, and reconfigurability [1,6]. The general steps in the simplest form involved in MPF are seen in Fig. 1. A modulator (E/O) modifies the RF in the CW laser light. The optical wave is transformed to the required spectral content after passing through one of the optical elements which include high-order MRR, ring-loaded MZI topologies, reflector-type MRR, phase-shifted Bragg gratings, and Brillion-active waveguide. After optical to electrical conversion, this optical signal was transformed into an electrical signal. Consequently, producing the output RF signal employing various optical receivers, therefore the optical filter transmission spectrum is measured.

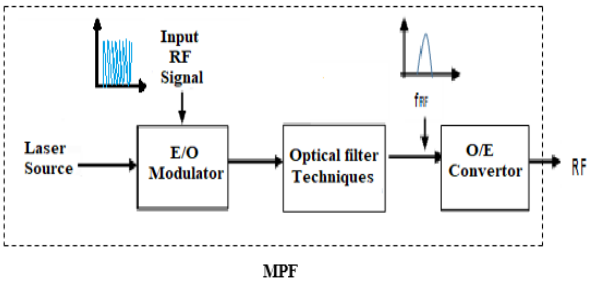

Figure (1): General steps concerned with tunable and Reconfigurable MPF.

3. Filter Design Technologies

By choosing the required spectral content and rejecting sideband signals, the MPF that made use of several technologies has shown the value of wide frequency tuning and reconfiguration in addition to its tolerance to electromagnetic interference. This work examines contemporary methods for designing microwave filters on multiple platforms such as: reflector-type MRR, Brillion-active waveguide, ring-assisted Mach-Zehender-Interferometer coupler, cascaded micro-ring resonator, and Bragg grating with phase shifts. Specifically, the MRR integrated with a MZI coupler technique's output characteristics are shown.

3.1 Microring Resonator

A common choice for tunable photonic filters is an MRR due to its scalability, small footprint, and straightforward structural design. When the phase shift and the coupling ratio are controlled with the tuning components, the bandwidth for MRRs is modulated [23 A bandpass MPF used an ultra-high-Q silicon MRR to provide an adjustable sub-gigahertz bandwidth [24] as shown in Fig. 2.

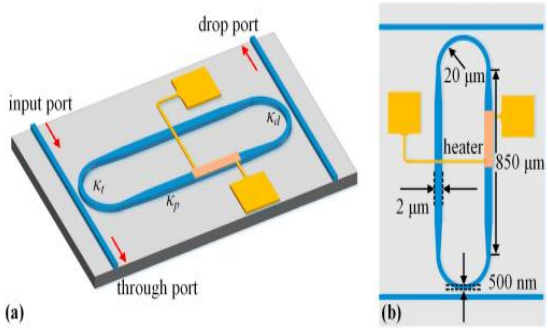

Figure (2): Diagrammatic representations of the MRR power field figures for the simulated fundamental TE mode. **(a)** Ultra-high-Q MRR layout; **(b)** MRR schematic top-view diagram [24].

The temperature dependency, size, practicality, standard complementary metal-oxide-semiconductor (CMOS) manufacturing technique, operating bandwidth, tunability, and practicality of the extreme narrowband MPF are all well-adjusted in this structure. It has a lot of potential uses in microwave frequency measurement and optoelectronic oscillators. This narrowband MPF breakthrough makes the prospect of MPF based silicon-system in the nearly futurity more encouraging [24]. A tunable MPF with an ultra-narrow band and excellent Q MRR is produced by combining the ultra-low coupling coefficients of the multimode ring resonator with the ultra-low loss of the silicon nitride waveguide [25]. MPF is based on a subwavelength grating-assisted microring resonator (SWG MRR), characterized by flat-top, strong sidelobe suppression, and wideband filter as shown in Fig. 3.

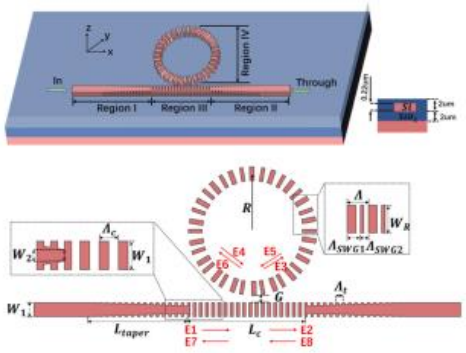

Figure (3): Diagrams showing the design parameters for the suggested double modulated grating assisted MRR **(a)** Perspective view in three dimensions. **(b)** Top view in two dimensions [27].

This feature allows for fabrication using electron beam lithography for additional experimental examination of the proposed wide-band filter output performance [26]. An adjustable bandpass MPF-based phase modulation with MRR as dual optical carriers is designed in order to lower the residue phase of the MRR, which limits the outside-of-band rejection ratio of conventional MPF based on phase modulation with a single optical carrier [27]. The technique of optical switchable filters between band pass and also band stop which used with MRR-related devices. On account of being very simple and accessible, also the device demonstrates high tunability for both band stop and band pass responses [28].

3.2 High-order MRR

Cascading various ring resonators produces sharper, narrower filtering at the cost of a higher insertion loss. The optimal coupling coefficients for cascaded MRRs can be used to generate configurable responses, which are necessary for many applications. Because of the microring waveguide's tiny minimum bending radius, MRR that functions as optical filters may be extremely compact, which makes it ideal for low power exhaustion [7]. Double-bus-coupled and cascaded silicon MRRs include an optical signal processor designed to handle the sideband and optical carrier signals independently. This system has high-quality characteristics, which makes the MPF very sensitive to waveguide propagation loss and is utilized in communication systems as optoelectronic integration technology develops [29]. A method of tiny notch MPF consists of integrated MRRs on an SOI chip as shown in Fig. 4 demonstrated. A filter improvement with a wide tuning range, high rejection ratio, low cost, very small footprint, shape-invariance, and shape factor during the tuning process is established [16,30].

Passband MPF built on a SOI platform with high-order MRR make flat top optical filter by adjusting each MRRs resonant wavelength [31,32]. Using cascaded photonic crystal (PHC) nanocavities in the suggested MPF is beneficial for the development of energy-efficient all-optical microwave systems on-chip. Consequently, it offers excellent rejection ratios, ultra-high tuning efficiency, and robust all-optical control [33].

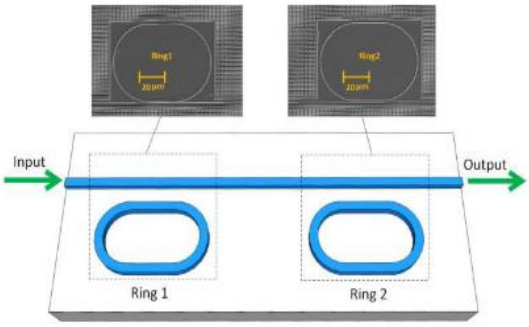

Figure (4): Illustration of the optical double-notch filter schematically [16].

Employing a low-loss Si3N4 circuit with cascaded MRR increased link gain, tuning rang, and decreased noise figures [20]. An intensity-consistent single-stage-adjustable cascaded microring (ICSSA-CM)-based phase-modulated flexible sideband cancellation technique is utilized to get rid of complex auxiliary devices and bias drift problems for a range of useful filter responses. This architecture for the silicon photonics platform produces broad-spectrum control flexibility, which has significant promise for next-generation wireless communication, radar, and sensor networks [34].

3.3 Reflective Type-MRR

A single microring resonator and two straight optical waveguides with a reflector connected to the

MRR's drop port make up an add-drop MRR with a reflector. Probably the reflector-type becomes a metal film, looped mirror, or grating coupler [14,35]. The reflective-type MRR, in comparison to conventional cascaded MRRs, reuses the identical MRR for two steps as a filter, this permits an on-chip system to be more stable. and decreases the chip magnitude and the number of microheaters that control the tunning process [15,36]. By adjusting the MRR's coupling coefficients, reflector-type enables reconfigurable intensity, group delay, and filtering with flat-top. Moreover, electro-optical modulation, XNOR/XOR optical logic operation, and wideband optical real time delay. This topology, as shown in Fig. 5, may enable new, compact, efficient designs for integrated reconfigurable or programmable microwave photonic systems [35].

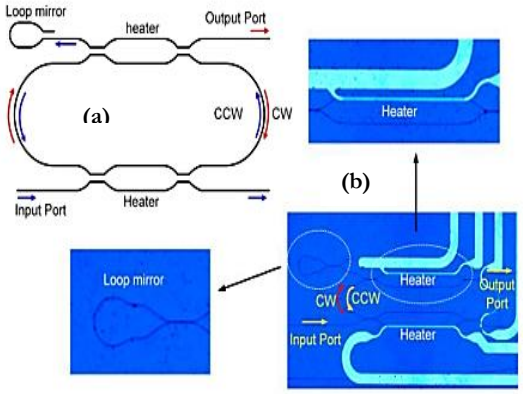

Figure (5): (a) Structure of the artificial reflective-type MRR and **(b)** microscope picture. Zoom-in views of the asymmetric Mach-Zehnder interferometer with a thermo-optic heater and the loop mirror are included in the insets [35].

3.4 Brillion-active Waveguide

RF photonic filtering is enhanced by the combination of passive design and Brillouin technology. Higher functionality, better performance, and compactness are achieved by combining both linear and nonlinear features. For the first time, a high-performance integrated photonic processing system utilizing photonic chips comprising passive ring resonators integrated with Brillouin-active waveguides is demonstrated. The nonlinear Brillouin-active waveguide and the passive over coupled OC ring resonator are shown individually in Fig. 6 by dashed boxes [37].

Using silicon multi-pole photonic filters improved performance by accessing long-lived phonons through designed Brillouin interactions, considerably increasing the silicon coherence periods. This type of filter uses linked defect modes in photonic crystal and acoustic mode engineering to build line geometries with an increase of 40 dB in out-of-band rejection over previous silicon-based filters [38]. This record performance is achieved by breaking the amplitude equality of a phase-modulated signal using a Brillouin dynamic grating (BDG) with an extremely narrow reflection spectrum of less than MHz. Thus, a single passband MPF with unprecedented performance—such as a wide spectrum range, great stability of center frequency drifting, and ultrahigh spectral resolution—was produced. [39]. Fig. 7 confirms a sub-kHz bandwidth MPF approach using a double-ring Brillouin fiber laser (DR-BFL).

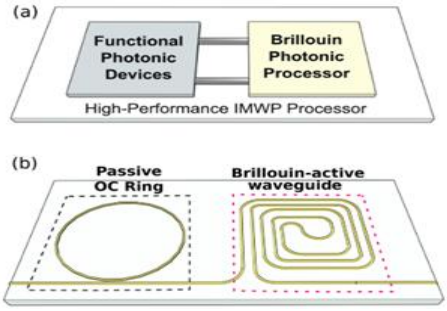

Figure (6): (a) A new class architecture of IMWP processors that integrates a Brillouin photonic processor on the same photonic chip. **(b)** The IMWP notch filter's architecture consists of a (OC) with a Brillouin waveguide that provides resonance for SBS gain [37].

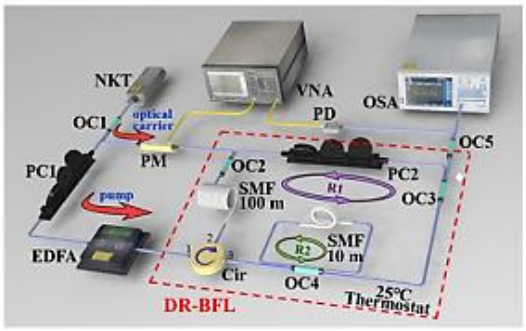

Figure (7): Configuration for an experiment. PM is for phase modulation; EDFA for erbium-doped fiber amplifier; Cir is a circulator; and NKT is an ultra-narrow linewidth fiber laser. PC, controller for polarization; PD stands for photodetector; OSA for optical spectrum analyzer; VNA stands for vector network analyzer; RF stands for radio frequency [40].

To generate a single passband narrow bandwidth MPF, the DR-BFL employed the Vernier effect with a single longitudinal mode laser output. To the best of knowledge, the MPF achieves the highest Q value. This architecture presents a novel concept for integrating high-precision signal extraction in next sensor or communication systems [40].

3.5 MRR assisted-MZI coupler

MRRs are often used in conjunction with MZI for several features. The phase shifter used with MRR-assisted MZIs can be very small due to the resonance in MRRs, resulting in significant power savings. Because of their compact footprints and simple structural design, MRRs and MZIs are frequently chosen to realize tunable photonic filters. When the phase shift and the coupling ratio are controlled by thermally adjusting the resonant wavelength, that give rise to the bandwidth for MRRs is modulated [23]. On a silicon-on-insulator (SOI) substrate, the MPF construction with MRR-integrated MZI is characterized by a wide tunable and reconfigurable bandpass MPF with a high rejection ratio [7], and also bandstop MPFs for processing sidebands individually [13]. This device could also achieve reduced crosstalk, a wide 3-dB bandwidth, and a rapid roll-off on the

band edges [41]. By using this method, the filter also achieves a high delay bandwidth and a moderate delay ripple. [42-43]. InP waveguides can be used to create an MPF constructive on the ring-assisted MZI (RAMZI) with significant filtering performances as shown in Fig. 8. The bandpass and band-stop functions of the filtering response can modify with flexibility and a small response time [21].

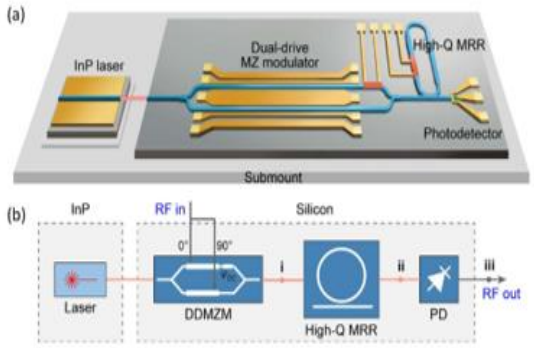

Figure (8): (a) The hybrid integrated MPF schematic diagram. **(b)** The principles governing the integrated MPF's bandpass/band-stop switchable filtering response [21].

This design found a workable way to achieve the larger frequency range, more compact size, and reduced power consumption that will enable a variety of RF applications, such as wireless communication and radar [44]. Because MZI can perform both infinite impulse response (IIR) and finite impulse response (FIR) filters, there are benefits to employing a Si_3N_4 waveguide device. It achieves a range of filter functions by combining rapid reconfigurability in an optical structure composed of both ring resonators and MZIs [19].

3.5.1 Analysis of the Output Characteristics of MRR Assisted-MZI Coupler

A symmetric MZI coupler linked to MRR satisfies high-Q resonators, which show the ability to modify the phase difference between the MZI coupler's two arms by varying the two-coupling coefficient in relation to the applied voltage in the microheaters [22]. As a result, MZIs show promise as an integrated coupler. For example, MZI modulators made of electro-optic polymer [45], a push-pull modulated MZI [46], and tunable and reconfigurable optical filters based on ring-assisted MZI coupler [7, 21,23]. We analyzed the phase modulation of the 2×2 MZI coupler [24] with high Q MRR, as the reason for studying the output characteristics as shown in Fig. 9.

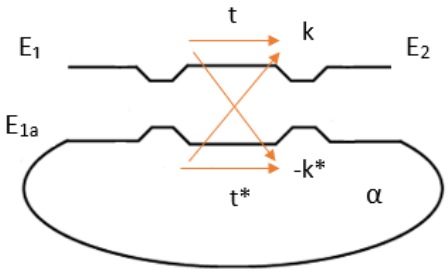

Figure (9): Diagram showing a MZI coupler coupled to a coupling-modulated microring.

Where α is the attenuation coefficient of the ring waveguide, The cross-coupling coefficient is denoted by k, and the self-coupling coefficient by t of the MZI coupler which is designed identically. The phase variation in the microheaters deposited in four arms of the two MZI couplers is expressed ΔØ. To resolve the interchange of optical power between optical waveguide MZI and ring waveguide, the coupling region proposed to a be lossless coupler, and this is represented in $t^2 + k^2 = 1$. Where t* and k*are the complex conjugate of the self and cross coupling coefficients, respectively, which are equal t*= -t and k*= -k. The electric field is slowly varying amplitude A, **t** is the time, and ω indicates the frequency of the optical signal which is expressed in:

$$E_1 = Ae\hat{}i\omega \boldsymbol{t} \quad \ldots (1)$$

and A is defined as:

$$A = (1 - t_1 t_2 \alpha e^{-i\emptyset}) \quad \ldots (2)$$

The intensity response was characterized by analyzing the electric field in the design according to the dynamic of microring resonator theory [47] shown in Fig. 9 from the input E_1 to the outport E_2:

$$E_2 = \left(t_1 e^{-i\Delta\emptyset_1} \times E_1 + k_1 e^{-i\Delta\emptyset_2} \times E_{1a}\right) \ldots (3)$$

The electric field inside the ring is represented by E_{1a}.

Design MRR with symmetric MZI coupler by the proposition of lossless coupling region, high-Q MRR was obtained and thus satisfy two conditions:

- minimizing the ring's attenuation as much as feasible (α =1),
- by applying the condition of critical coupling when the coupling at steady-state value t_0 is equal to the attenuation $|t_0| = \alpha$,

It's worth mentioning that the over coupling and under coupling condition have come true when $|t_0| < \alpha$ and $|t_0| > \alpha$, respectively [22]. In addition, by using the method of adjustable coupling strength, rather than the refractive index or ring loss, it is possible to create modulation bandwidths with high-quality factors, which operate at frequencies significantly higher than the resonator linewidth [48]. Thus, the dynamical transmission T(**t**) could be expressed [47] as;

$$T(\boldsymbol{t}) \equiv \frac{E_2}{E_1} = \left[t + \frac{k(\boldsymbol{t})}{k(\boldsymbol{t}-\tau)}\, \alpha\, e^{i(\theta+\Delta\emptyset)[t(\boldsymbol{t}-\tau)T(\boldsymbol{t}-\tau)-1\,]}\right] \ldots (4)$$

Where τ, and θ represent the propagation time coupler, and propagation phase shift, respectively. To solve Eq. (4), It can be written as a second-kind Fredholm integral equation, which resolves the Neuman series solution;

$$T(\boldsymbol{t}) = t(\boldsymbol{t}) - \frac{\kappa(\boldsymbol{t})}{\kappa(\boldsymbol{t}-\tau)}\alpha(\boldsymbol{t})\, exp[-i(\theta + \Delta\emptyset)] + \int_{-\infty}^{\infty} \frac{\kappa(t'+\tau)}{\kappa(t')}\alpha(t'+\tau)t(t') \exp[-i\theta(t'+\tau)]\, \delta[t' - (\boldsymbol{t}-\tau)]\, T(t')dt' \quad \ldots (5)$$

From Eq. (5), the dynamical transmission becomes equal to the static state transmission by assuming α(**t**), k(**t**), t(**t**), and θ(**t**) recurrent with a period equal to the propagation time. And so, by removing time independent through applying conditions of critical coupling when $t_0 = \alpha$ and $\alpha = 1$, the static stat transmission Tss are satisfied;

$$T_{ss} = \frac{[t_0 - \alpha e^{-i(\theta+\Delta\emptyset 1)}]}{[1-\alpha t_0 * e^{-i(\theta+\Delta\emptyset 2)}]} \quad \dots (6)$$

$$t' = \frac{-k_0 * k'}{t_0 *} \quad \dots (7)$$

Where t` and k' are the intensity of the coupling strength, k_0 and t_0 are the steady-stat values of two coupling coefficients. Based on the previous Eq. (6) and (7), the high-Q transmission design was examined through the following equation:

$$TQ = T_{ss} + t' \quad \dots (8)$$

$$TQ = \left[\frac{[t_0 - \alpha e^{-i(\theta+\Delta\emptyset 1)}] - \frac{k_0 * k'}{t_0 *}}{[1-\alpha t_0 * e^{-i(\theta+\Delta\emptyset 2)}]}\right] \quad \dots (9)$$

When there is no resonance in the input and the ring is critically connected, and the output of the high-Q resonator is given as;

$$|TQ|^2 = |T_{ss}|^2 + k' \frac{2k_0\left[1 + \frac{\alpha}{|t_0|} sin\,(\theta + \Delta\phi_1)\right]}{1 + \alpha^2|t_0|^2 + 2\alpha|t_0| sin\,(\theta + \Delta\phi_2)}$$
$$+|k'|^2 \frac{\left|\frac{k_0}{t_0}\right|^2}{1 + \alpha^2|t_0|^2 + 2\alpha|t_0|\,sin(\theta + \Delta\phi_2)} \quad \dots (10)$$

$$|TQ|^2 = |T_{ss}|^2 + k'(G_1) + |k'|^2 G_2 \quad \dots (11)$$

From Eq. (11) its noticeable there was an enhancement in the gain represented in G_1 and G_2 arising from field and intensity coupling strength k' and $|k'|^2$, respectively. At resonance input, G_1 and G_2 represent in these equations;

$$G_1 = \frac{2k_0\left(1 - \frac{\alpha}{|t_0|}\right)}{(1-\alpha|t_0|)^2} \quad \dots (12)$$

$$G_2 = \frac{\frac{|k_0|^2}{|t_0|^2}}{(1-\alpha|t_0|)^2} \quad \dots (13)$$

$$\boldsymbol{L} = \left|\frac{G_1}{G_2}\right| \quad \dots (14)$$

The linearity parameter **L** describes linear change in high-Q transmission $|TQ|^2$due to the coupling strength $|k'|$ and $|k'|^2$which represents the gain factors G1 and G2, and thus with regard to the applied voltage in two arms of MZI that causes phase variation [22,49]. Fig. 10 represented inserting these three Eq. (12,13,14) through MATLAB software, the relationship between the gain factors in two different valued of α could sketched. Where Fig. 10a and b are demonstrated the relationship of the two conditions that satisfied high-Q resonator which causes the variation in output gain. The value for $|t_0|$ in G_1 and G_2 is lower in the smaller value of attenuation α. In Fig. 10c illustrates the linearity parameter in three situations; for $\mathbf{L} \ll 1$, the attenuation is greater than the $|t_0|$ and over-coupling conditions satisfied $|t_0| < \alpha$, thus the intensity of coupling strength $|k'|^2$are dominate. When **L**= 0 at critical coupling conditions $|t_0| = \alpha$, G_1= 0, $|T_{ss}|^2$= 0 where only $|k'|^2$are dominate. And $\mathbf{L} \geq 1$ to obtain low-loss resonators and that will satisfy the under-couple condition where $|t_0| > \alpha$.

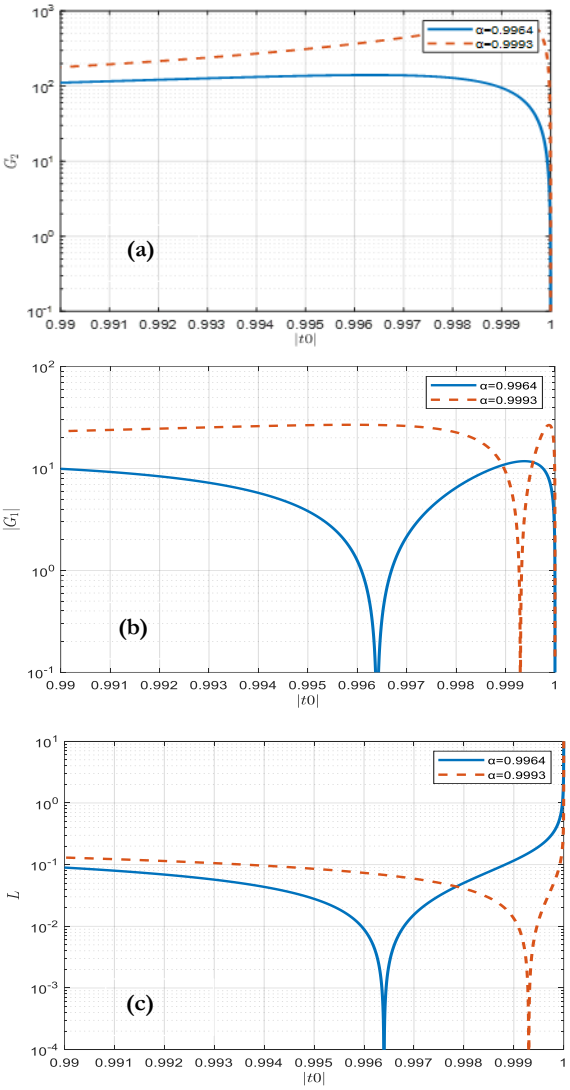

Figure (10): Various values of $|t_0|$ for input resonant in; **(a)** $|G_1|$, the gain parameter related to the $|k'|$. (b) G_2, the gain parameter related to the $|k'|$. **(c)** The linearity parameter **L**.

From all above, the MZI coupler integrated with MRR was showed liner change in the transmission spectrum due to the small variations in coupling strength with respect to the voltage applied in the two arms of MZI. Which showed a good specification to examine the characteristics of coupling modulated microrings with MZI couplers. The research demonstrates that combining a microring with a MZI is a great way to take the advantages of both resonant and nonresonant modulators at the same time.

3.6 Other Design Technology

An MRR with a single ring covered in Bragg grating makes the filter a silicon-based wideband filter

with excellent side lobe suppression. The subwavelength grating (SWG) waveguide, which consists of two identical-period gratings with differing filling factors to cause refractive index change in the direction of transmission, is what creates the Bragg grating in microring. Hence, wider bandwidth, higher sidelobe suppression, and infinite FSR can be obtained in this device [26]. An article showed how to make a programmable SOI on-chip filter using a four-tap finite impulse response topology. The photonic filter might be programmed because thermal heaters vary the amplitude and phase of each tap. It also demonstrated the tuneable center wavelength, bandwidth, and passband form of the filter.

Benefits of this project include its compact design and its ability to integrate with electronics [50]. Particular attention has been paid to the description of novel optoelectronic oscillator or MPF techniques that are thought to solve the serious shortcomings of traditional systems. With the use of these methods, high-performance optical filtering-assisted MWP signal processing and sensing will advance more quickly [5]. Table (1) showed results of MFPs in different technologies.

Table (1): Comparison of Different Technologies Results Involved in Tunable and Reconfigurable MPFs

Technology	Platform	Filter Type	Reconfigure (GHz)	Rejection Ratio(dB)	Tuning Range (GHz)
MRR&MZI [21]	InP	Bandpass Bandstop	0.36	40>	3-25
MRR [24]	Si	Bandpass	0.17	23.7	2-18.4
ICSSA-CM [34]	Si	Bandpass	30	60	0.22
MRR [18]	SOI	Bandpass Bandstop	0.97-0.84	62	5-35
DR-MZIs [19]	Si_3N_4	Bandpass	0.79-8.87	20	2-9
R-type MMR [32]	SOI	Bandpass Bandstop	3-78	60>	37.7-95.2
DR-BFL [40]	SMF	Bandpass	114		10.735

4. Conclusions:

In both present-day and future wireless communication systems, tunable and reconfigurable microwave filters are essential components. This work presents a broad overview of current methods used in the design of microwave filters. Different technologies are used to compare the parameters involved in filter designs, and the findings are summarized. The methods utilized to develop and implement filters with specified frequency and bandwidth-adjusting capabilities were the main emphasis of the workshop. Some of the uses for microwave filters were also covered in this publication. Furthermore, the output characteristics of the MRR assisted MZI coupler technique were demonstrated. The following are some salient features of the primary technological issues of today.

1) Creating strategies and processes to produce stable filters with high Q values.
2) Creating more condensed methods for obtaining complicated and negative coefficient filters. Research on innovative MZI and electro-absorption modulator structures is necessary for this.
3) Improving the methods that result in filter tunability and reconfigurability through employing Brillion technology, GC-reflector, or cascaded MRR.
4) Overcoming the scattering and losing effects in filters with compactness considering circuit integration.

Worth mentioning, Fig. 11 proposes the principles of integrating new innovative concepts to address emerging challenges, which might open the way for next-generation photonic filters with enhanced performance and related versatility. Future Research Direction.

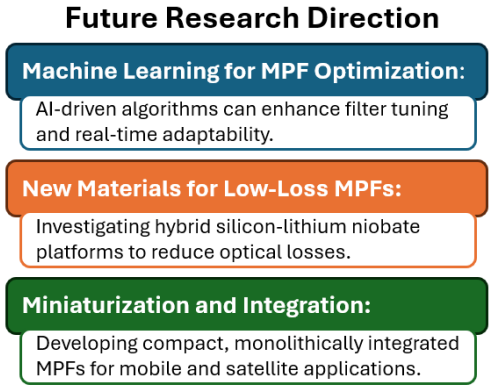

Figure (11): The suggested future research directions for optimizing MPFs in next-generation communication systems.

5. References:

[1] C. José, O. Beatriz, and P. Daniel, "A tutorial on microwave photonic filters," J. Light. Technol., vol. 24, no. 1, pp. 201–229, 2006.
[2] X. Zhu, B. Crockett, C. M. L. Rowe, and J. Azaña, "Broadband and Fine-resolution Microwave Photonic Filtering with High-Speed Electronic Reconfigurability," Optica Publishing Group., pp. 4–6, 2023.
[3] G. N. Saddik, R. S. Singh, and E. R. Brown, "Ultra-wideband multifunctional communications/radar system," IEEE Transactions on Microwave Theory and Techniques, vol. 55, no. 7. pp. 1431–1436, 2007.
[4] L. Xu et al., "A highly sensitive and precise temperature sensor based on optoelectronic oscillator," Opt. Commun., vol. 483, 2021.
[5] L. Li, X. Yi, S. Song, S. X. Chew, R. Minasian, and L. Nguyen, "Microwave photonic signal processing and sensing based on optical filtering," Applied Sciences (Switzerland), vol. 9, no. 1. 04, 2019.
[6] D. Marpaung, C. Roeloffzen, R. Heideman, A. Leinse, S. Sales, and J. Capmany, "Integrated microwave photonics,". 2012.

[7] Y. Liu, Y. Chen, L. Wang, Y. Yu, Y. Yu, and X. Zhang, "Tunable and Reconfigurable Microwave Photonic Bandpass Filter Based on Cascaded Silicon Microring Resonators," J. Light. Technol., vol. 40, no. 14, pp. 4655–4662, 2022.
[8] V. Mishra and S. Gupta, "Microwave Photonic Filter: A Systematic Literature Review," IJARCCE, vol. 6, no. 5, pp. 628–634, 2017.
[9] J. Capmany, D. Pastor, and B. Ortega, "New and flexible fiber-optic delay-line filters using chirped bragg gratings and laser arrays," IEEE Trans. Microw. Theory Tech., vol. 47, no. 7 PART 2, pp. 1321–1326, 1999.
[10] G. N. Saddik, R. S. Singh, and E. R. Brown, "Ultra-wideband multifunctional communications/radar system," IEEE Transactions on Microwave Theory and Techniques, vol. 55, no. 7. pp. 1431–1436, 2007.
[11] J. Capmany, D. Pastor, A. Martinez, B. Ortega, and S. Sales, "Microwave photonic filters with negative coefficients based on phase inversion in an electro-optic modulator," Opt. Lett., vol. 28, no. 16, p. 1415, 2003.
[12] R. Waterhouse and D. Novack, "Realizing 5G: Microwave photonics for 5g mobile wireless systems," IEEE Microw. Mag., vol. 16, no. 8, pp. 84–92, 2015.
[13] D. Zhang, X. Feng, X. Li, K. Cui, F. Liu, and Y. Huang, "Tunable and reconfigurable bandstop microwave photonic filter based on integrated microrings and mach-zehnder interferometer," J. Light. Technol., vol. 31, no. 23, pp. 3668–3675, 2013.
[14] M. Huang, S. Li, Z. Yang, and S. Pan, "Analysis of a flat-top optical ring resonator," Opt. Commun., vol. 451, pp. 290–295, 2019.
[15] M. Huang, S. Li, M. Xue, L. Zhao, and S. Pan, "Flat-top optical resonance in a single-ring resonator based on manipulation of fast- and slow-light effects," Opt. Express, vol. 26, no. 18, p. 23215, 2018.
[16] S. Song, S. X. Chew, X. Yi, L. Nguyen, and R. A. Minasian, "Tunable single-passband microwave photonic filter based on integrated optical double notch filter," J. Light. Technol., vol. 36, no. 19, pp. 4557–4564, 2018.
[17] L. Xu et al., "Silicon-on-insulator-based microwave photonic filter with widely adjustable bandwidth," Photonics Res., vol. 7, no. 2, p. 110, 2019.
[18] W. Jiang et al., "Optical filter switchable between bandstop and bandpass responses in SOI wafer," IEEE Photonics Technol. Lett., vol. 32, no. 17, pp. 1105–1108, 2020.
[19] Q. Sun, L. Zhou, L. Lu, G. Zhou, and J. Chen, "Reconfigurable High-Resolution Microwave Photonic Filter Based on Dual-Ring-Assisted MZIs on the Si3N4 Platform," IEEE Photonics J., vol. 10, no. 6, 2018.
[20] O. Daulay, R. Botter, and D. Marpaung, "On-chip programmable microwave photonic filter with an integrated optical carrier processor," OSA Contin., vol. 3, no. 8, p. 2166, 2020.
[21] Y. Tao et al., "Hybrid-integrated high-performance microwave photonic filter with switchable response," Photonics Res., vol. 9, no. 8, p. 1569, 2021.
[22] W. D. Sacher and J. K. S. Poon, "Characteristics of microring resonators with waveguide-resonator coupling modulation," J. Light. Technol., vol.
[23] Y. Xie et al., "Thermally-Reconfigurable Silicon Photonic Devices and Circuits," IEEE J. Sel. Top. Quantum Electron., vol. 26, no. 5, 2020.
[24] H. Qiu et al., "A continuously tunable sub-gigahertz microwave photonic bandpass filter based on an ultra-high-Q silicon microring resonator," J. Light. Technol., vol. 36, no. 19, pp. 4312–4318, 2018.
[25] H. Yang, J. Li, G. Hu, B. Yun, and Y. Cui, "Hundred-megahertz microwave photonic filter based on a high Q silicon nitride multimode microring resonator," OSA Contin., vol. 3, no. 6, p. 1445, 2020.
[26] C. Fang, V. R. Shrestha, I. A. Ukaegbu, G. Ren, S. Pan, and B. Nakarmi, "Ultra-compact wideband filter with sidelobe suppression based on double modulated grating-assisted microring resonator," Opt. Contin., vol. 1, no. 4, p. 623, 2022.
[27] J. Li, P. Zheng, G. Hu, R. Zhang, B. Yun, and Y. Cui, "Performance improvements of a tunable bandpass microwave photonic filter based on a notch ring resonator using phase modulation with dual optical carriers," Opt. Express, vol. 27, no. 7, p. 9705, 2019.
[28] W. Jiang et al., "Optical filter switchable between bandstop and bandpass responses in SOI wafer," IEEE Photonics Technol. Lett., vol. 32, no. 17, pp. 1105–1108, 2020.
[29] Z. Zhang, B. Huang, Z. Zhang, C. Cheng, and H. Chen, "Microwave photonic filter with reconfigurable and tunable bandpass response using integrated optical signal processor based on microring resonator," Opt. Eng., vol. 52, no. 12, p. 127102, 2013.
[30] J. Dong et al., "Compact notch microwave photonic filters using on-chip integrated microring resonators," IEEE Photonics J., vol. 5, no. 2, 2013.
[31] L. Xu et al., "Silicon-on-insulator-based microwave photonic filter with widely adjustable bandwidth," Photonics Res., vol. 7, no. 2, p. 110, 2019.
[32] F. M. Geremew and S. Talabattula, "Performance analysis of reconfigurable multifunctional photonic filters using triple coupled microring resonators," Opt. Commun., vol. 486, 2021.
[33] L. Liu and S. Liao, "Low-Power Active Tunable Microwave Photonic Filter Using Photonic Crystal Nanocavities," IEEE Photonics Technol. Lett., vol. 32, no. 16, pp. 999–1002, 2020.
[34] Z. Tao et al., "Highly reconfigurable silicon integrated microwave photonic filter towards next-generation wireless communication," Photonics Res., vol. 11, no. 5, pp. 682–694, 2023.

[35] S. Pan, Z. Tang, M. Huang, and S. Li, "Reflective-Type Microring Resonator for On-Chip Reconfigurable Microwave Photonic Systems," IEEE J. Sel. Top. Quantum Electron., vol. 26, no. 5, 2020.
[36] F. M. Geremew and T. Srinivas, "Reflective coupled microring resonators for reconfigurable photonic systems: Performance analysis," Results Opt., vol. 5, p. 100111, 2021.
[37] Y. Liu et al., "Integration of Brillouin and passive circuits for enhanced radio-frequency photonic filtering," APL Photonics, vol. 4, no. 10, 2019.
[38] S. Gertler, E. A. Kittlaus, N. T. Otterstrom, and P. T. Rakich, "Tunable microwave-photonic filtering with high out-of-band rejection in silicon," APL Photonics, vol. 5, no. 9, 2020.
[39] H. S. Wen et al., "Ultrahigh spectral resolution single passband microwave photonic filter," Opt. Express, vol. 29, no. 18, p. 28725, 2021.
[40] L. Wang et al., "Microwave photonic filter with a sub-kHz bandwidth based on a double ring Brillouin fiber laser," Opt. Lett., vol. 47, no. 16, p. 4143, 2022.
[41] F. Zhou, X. Gu, G. Qian, Y. Kong, and T. Chen, "Band-pass photonic filter based on a ring resonator assisted with an asymmetric MZI," Proc. SPIE, p. 232, 2020.
[42] W. Shan et al., "Broadband continuously tunable microwave photonic delay line based on cascaded silicon microrings," Opt. Express, vol. 29, no. 3, p. 3375, 2021.
[43] Y. Chen et al., "Reconfigurable second-order optical all-pass filter," Nanophotonics, vol. 11, no. 13, pp. 3115–3125, 2022.
[44] J. S. Fandiño, P. Muñoz, D. Doménech, and J. Capmany, "A monolithic integrated photonic microwave filter," Nat. Photonics, vol. 11, no. 2, pp. 124–129, 2017.
[45] D. Chen, H. R. Fetterman, A. Chen, W. H. Steier, L. R. Dalton, W. Wang, and Y. Shi, "Demonstration of 110 GHz electro-optic polymer modulators," Appl. Phys. Lett., vol. 70, no. 25, pp. 3335–3337, 1997.
[46] F. Koyama and K. Iga, "Frequency chirping in external modulators," J. Lightw. Technol., vol. 6, pp. 87–93, 1988.
[47] W. D. Sacher and J. K. S. Poon, "Dynamics of microring resonator modulators," Opt. Express, vol. 16, no. 20, p. 15741, 2008.
[48] E. G. Turitsyna and S. Webb, "Simple design of FBG-based VSB filters for ultra-dense WDM transmission ELECTRONICS LETTERS 20th January 2005," Electron. Lett., vol. 41, no. 2, pp. 40–41, 2005.
[49] A.A. Al-mfrji, S.K. Tawfeeq, R.S. Fyath, "Design guideline for plasmonic 16-QAM optical modulator," Photonics and Nanostructures - Fundamentals and Applications, vol. 21, pp. 82–106, 2016.
[50] S. Liao, Y. Ding, C. Peucheret, T. Yang, J. Dong, and X. Zhang, "Integrated programmable photonic filter on the silicon-on-insulator platform," Opt. Express, vol. 22, no. 26, p. 31993, 2014.